OCEANOGRAPHY

Decadal oscillations in the ocean's largest oxygen-deficient zone

N. N. Duprey[1]*, A. D. Foreman[1], J. D. Carriquiry[2]†, C. D. Charles[3], S. C. Sanchez[4], H. Vonhof[1], F. Rubach[1], R. Rabenstein[5], M. Rohr[6], H. Reyes-Bonilla[7], D. Marconi[8], D. M. Sigman[8], G. H. Haug[1,9], A. Martínez-García[1]*

The impact of global warming on the ocean's oxygen-deficient zones (ODZs) is uncertain, partly because of a lack of data on past changes. We report monthly resolved records of coral skeleton–bound nitrogen isotopes (CS-$\delta^{15}N$) to reconstruct denitrification in the Eastern Tropical North Pacific (ETNP) ODZ over the last 80 years. The data indicate strong decadal variation in ETNP denitrification, with maxima during the cool North Pacific phase of Pacific Decadal Variability. The maxima in denitrification (and thus oxygen deficiency) were likely due to stronger upwelling that enhanced productivity leading to greater oxygen demand in the thermocline. Prior findings of multidecadal-to-centennial ODZ trends were likely biased by this variability. ODZ evolution over the next century will depend on how global warming interacts with the decadal oscillations.

Global warming in the coming decades has been predicted to drive the expansion of the oxygen-deficient zones (ODZs, O_2 < 4.5 μmol.kg^{-1}) (*1*), which could have far-reaching consequences for both pelagic and coastal ecosystems (*2*). Most of the current concerns focus on the Eastern Tropical North Pacific (ETNP) ODZ, which hosts over 95% of the world's suboxic water volume and plays a central role in the ocean's biogeochemistry (Fig. 1A). Compiled measurements suggest a decline, since 1960, in dissolved oxygen concentration at intermediate depths (100 to 1000 m) in the Equatorial Pacific (*1*, *3*), along the California coast (*4*) and in the ETNP ODZ core region (*5*). However, the available instrumental dissolved oxygen observations are sparse. In a number of numerical models, simulations of global warming suggest a more complex response of O_2 concentration, with tropical intermediate-depth oxygen declining on average but the ODZs contracting (*6*). However, across numerical models, the direction of ODZ response varies, some simulating an expansion of the ODZs (*7*, *8*), and others, a contraction (*6*, *9*). Better data on the recent history of the ODZs could help to clarify their relationship with climate.

Nitrogen isotopes and water column denitrification

Measurements of the stable nitrogen isotopic composition ($\delta^{15}N$) of marine archives can provide continuous records of oxygen deficiency both before and during the instrumental period (*10*) {$\delta^{15}N = [(^{15}N/^{14}N_{sample})/(^{15}N/^{14}N_{reference})] - 1) * 1000$, where the atmospheric N_2 (AIR) is the universal reference (‰ vs. AIR)}. In ODZs, heterotrophic bacteria in the water column respire by denitrification, wherein nitrate (NO_3^-) substitutes for oxygen (O_2) as the electron acceptor in the catabolic oxidation of organic matter. This water column denitrification (WCD) preferentially consumes the light isotope of nitrogen (^{14}N) (*11*), elevating the $\delta^{15}N$ of the remaining nitrate pool above the mean global pycnocline nitrate $\delta^{15}N$ [~6.2‰, (*12*)]. In oligotrophic settings, this ^{15}N-enriched nitrate pool is upwelled to the surface and fully assimilated by primary producers. Consequently, the $\delta^{15}N$ values of net community production and particulate organic matter export reflect the $\delta^{15}N$ of the nitrate supplied to the euphotic zone from the underlying thermocline and, thus, provides a proxy for WCD in ODZs (*13*). The high-$\delta^{15}N$ signal of the ODZs is also transported far beyond their boundaries (*14*), ultimately elevating the $\delta^{15}N$ of the entire ocean's nitrate reservoir (*15*). The high-$\delta^{15}N$ nitrate from the ETNP ODZ survives far westward into the central tropical zone within the "shadow zone" of North Pacific subtropical thermocline (*16*), evident as nitrate $\delta^{15}N$ above 10‰ at 150° to 160°W (Fig. 1B).

Different archives offer the opportunity to generate continuous reconstructions of past changes in ODZ denitrification. The $\delta^{15}N$ of sinking organic matter is reflected in the skeleton of proteinaceous and stony deep-sea corals that feed on particulate matter from the surface (*17*, *18*). In sites of higher organic matter preservation (i.e., owing to low bottom water oxygen), sedimentary organic matter can also record the $\delta^{15}N$ of N exported from surface waters (*10*). The $\delta^{15}N$ of Hawaiian proteinaceous corals, Baja California sediments (Pescadero and Soledad basins) and California margin sediments (Santa Monica basin) indicate a steady decline in $\delta^{15}N$ over the period 1[illegible] to 2000, followed by a rise in the sedim[illegible] $\delta^{15}N$ records from the year 2000 onward (Fig. 2). The changes in the Baja California $\delta^{15}N$ have been interpreted as a reflection of WCD in the ETNP (*10*), whereas Santa Monica Basin $\delta^{15}N$ has the potential to record changes in both ETNP WCD and the northward transport of high-$\delta^{15}N$ ETNP nitrate by the California Undercurrent (*19*). ODZ extent and WCD rate are both enhanced by wind-driven upwelling, which increases biological production of sinking organic matter and thus oxygen demand in the subsurface (*10*). The decline in the ETNP sediment $\delta^{15}N$ over the period 1940 to 2000 is interpreted as a reduction in WCD owing to a progressive weakening of the easterly winds, whereas the $\delta^{15}N$ rise from 2000 onward is interpreted as an invigoration of WCD in response to a wind strengthening (*10*).

A dependence of WCD in the ETNP ODZ on the easterly winds implies that the intensity of WCD may respond to decadal climatic variability in the Pacific. However, the deposition rate of organic sedimentary N and the slow growth rate of deep-sea corals largely preclude the reconstruction of interannual and decadal processes with these archives, and direct water column measurements of dissolved oxygen and of other redox-sensitive parameters through time are sparse.

Nitrogen isotope records from stony corals

In this work, we measured the $\delta^{15}N$ of aragonite skeleton–bound organic matter (coral skeletal–bound $\delta^{15}N$, or CS-$\delta^{15}N$) in shallow-water scleractinian ("stony") corals to gain new insight into the recent history of WCD in the ETNP ODZ. Using the "oxidation-denitrifier" method, we measured CS-$\delta^{15}N$ at a subannual resolution (*20*, *21*). Unlike deep-sea proteinaceous corals, shallow tropical scleractinian corals live in sunlit surface waters, where they ingest plankton growing on the nitrate supply from below (*22*) or assimilate nitrogen directly through their photosymbionts (*23*). As a consequence of their nitrogen acquisition, their tissues and skeleton-bound organic matter reflect the $\delta^{15}N$ of the nitrate supply to the euphotic zone from the shallow subsurface (*24*), making CS-$\delta^{15}N$ a potential archive of past changes in WCD. CS-$\delta^{15}N$ is protected from alteration associated with microbial respiration and other diagenetic processes (*25*), in contrast to the vulnerability of bulk sedimentary $\delta^{15}N$ to diagenesis and exogenous inputs (*26*). Another advantage of coral skeleton is that many genera (such as *Porites*) display annual density bands, permitting the construction of high-resolution records of CS-$\delta^{15}N$ (*27*, *28*), with the potential to reconstruct rapid changes in ocean suboxia over the past century.

We generated seven high-resolution (quarterly to monthly) CS-$\delta^{15}N$ records from the coral

[1]Max Planck Institute for Chemistry (Otto Hahn Institute), Mainz, Germany. [2]Terracoast Environmental Consultants, Ensenada, Baja California, México. [3]Scripps Institution of Oceanography, La Jolla, CA, USA. [4]Department of Atmospheric and Oceanic Sciences, University of Colorado, Boulder, CO, USA. [5]Messel Research and Mammalogy, Senckenberg Research Institute, Frankfurt am Main, Germany. [6]Rohr Foundation, Dallas, TX, USA. [7]Departamento Académico de Ciencias Marinas Y Costeras, Universidad Autónoma de Baja California Sur, La Paz, Baja California Sur, Mexico. [8]Department of Geosciences, Princeton University, Princeton, NJ, USA. [9]Department of Earth and Planetary Sciences (D-EAPS) ETH Zürich Sonneggstrasse 5, Zürich, Switzerland.
*Corresponding author. Email: n.duprey@mpic.de (N.N.D.); a.martinez-garcia@mpic.de (A.M.G.)

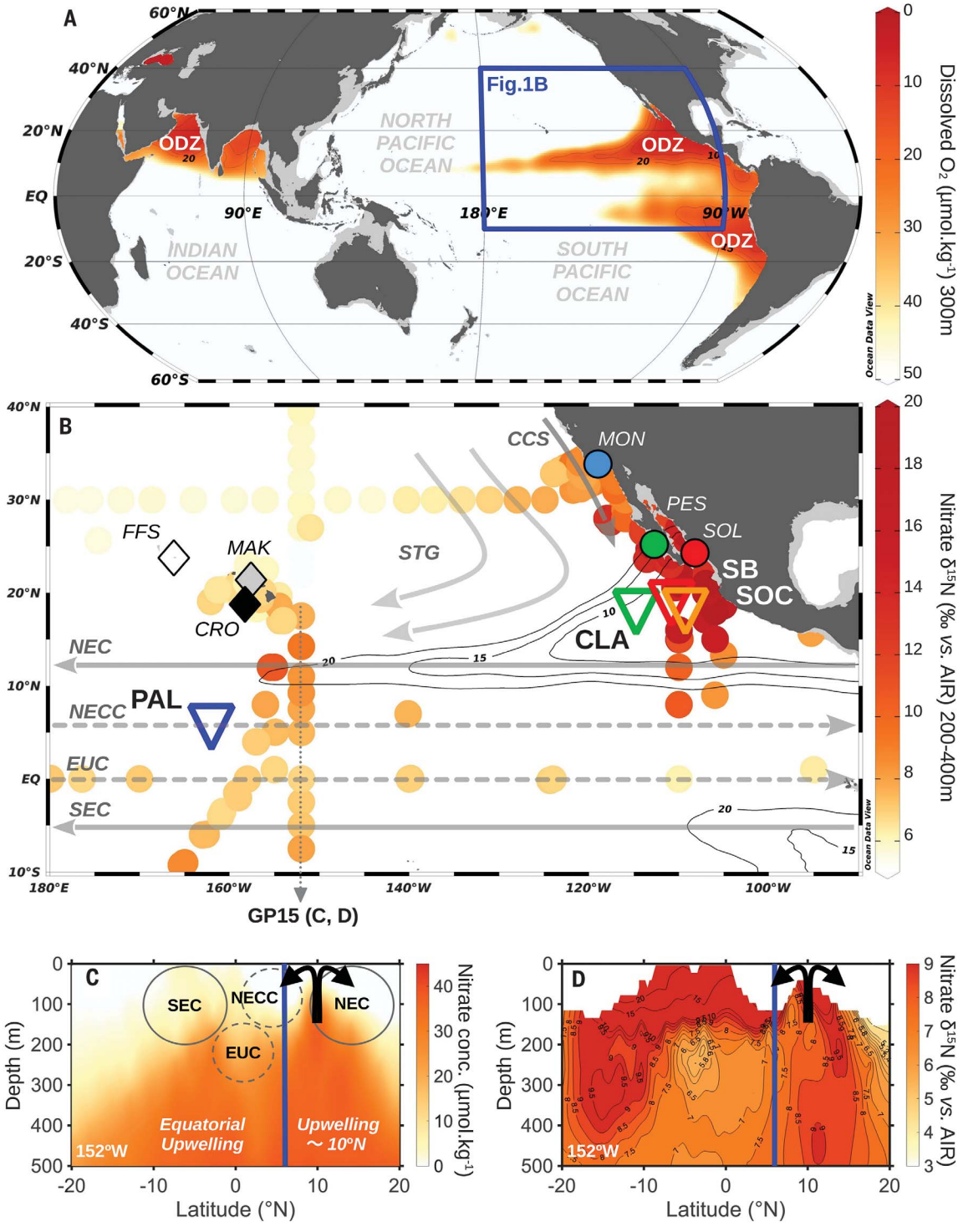

Fig. 1. Sites of major ODZs and coral cores used in this study, in the context of thermocline dissolved oxygen concentration, water column nitrate $\delta^{15}N$ and previously published $\delta^{15}N$ records from sediment and proteinaceous corals. (**A**) Location of the three major ODZs on the planet (at the core of the orange regions, shaded according to dissolved oxygen concentration). This study focuses on the largest ODZ located in the ETNP (blue box). (**B**) Corresponds to the blue-boxed region in (A). Ocean circulation in the thermocline and the location of the ETNP ODZ (dissolved oxygen contour lines in micromole per kilogram). Existing $\delta^{15}N$ records from sediment (MON, Santa Monica; SOL, Soledad; PES, Pescadero), proteinaceous corals (MAK, Makapuu; FFS, French Frigate Shoals; CRO, Cross Seamount), new records from shallow scleractinian corals (PAL, Palmyra Atoll; SOC, Socorro Island; CLA, Clarion Island; SB, San Benedicto Island) and nitrate $\delta^{15}N$ data measured at 200- to 400-m depth from (*29*) and (*33*) were used to investigate the dynamics of the ODZ over the past century. $\delta^{15}N$ is expressed as per mille, normalized versus atmospheric N_2 (‰ vs. AIR). (**C** and **D**) Depth sections focused on the thermocline (0 to 500 m) versus latitude {from 20°S to 20°N along 152°W [US GEOTRACES Pacific Meridional Transect – GP15 (*29*)]}; (C) shows nitrate concentration (shading) and the location of the currents shown in (B) (dashed contours = eastward flow), and (D) shows nitrate $\delta^{15}N$ (shading and contours). Data are shown here only for samples of 0.3-µM nitrate or greater. The black arrows in (C) and (D) indicate the upwelling within the path of the NEC that convey the ODZ signal to the reefs of Palmyra Atoll (blue line). STG, subtropical gyre; CCS, California Current System; EUC, Equatorial Undercurrent; SEC, South Equatorial Current.

genus *Porites* (table S1) spanning the ETNP ODZ and nearby waters. Two CS-$\delta^{15}N$ records are from the core of the ODZ: San Benedicto Island (1956 to 1998; Fig. 1B, red triangle) and Socorro Island (1992 to 2016; Fig. 1B, orange triangle). A third record (1940 to 1998) is from Clarion Island, at the northern margin of the ODZ (Fig. 1B, green triangle). Four additional records (1997 to 2016) are from Palmyra Atoll in the Central Pacific (Fig. 1B, blue triangle). Palmyra receives little nitrate from the equatorial upwelling, which is exhausted southward of ~2.5°N

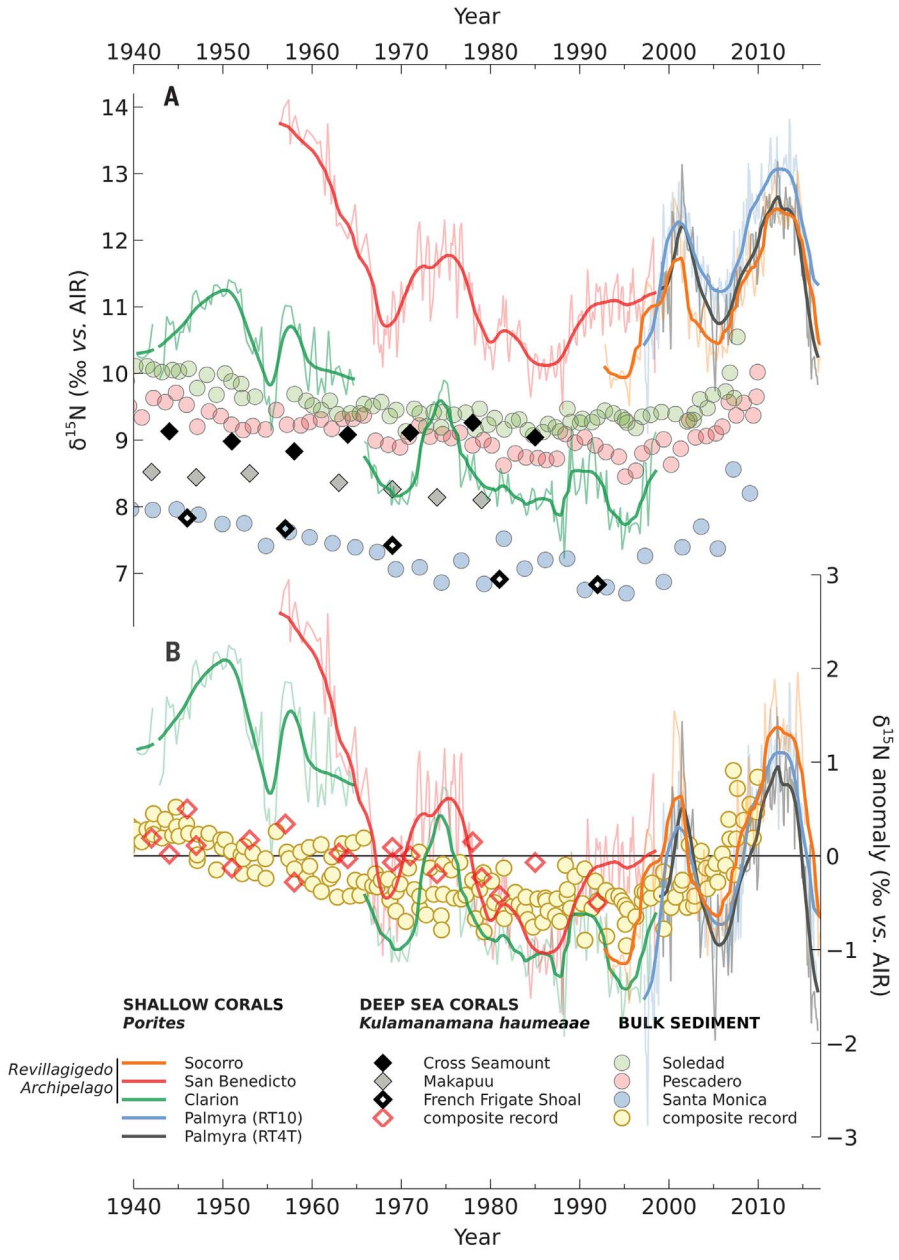

Fig. 2. Compilation of existing and new $\delta^{15}N$ records from bulk sediment (*10*), from the skeleton of the deep-sea coral *Kulamanamana haumeaae* (*17*) and of the shallow tropical coral genus *Porites* from the Eastern and Central Tropical Pacific. (**A**) Sediment and coral $\delta^{15}N$ records are bounded by the global mean pycnocline nitrate $\delta^{15}N$ of ~6.2‰ and the value measured within the core of the ODZ (≥15‰), indicating that all locations are influenced to some degree by nitrate originating from the ODZ. (**B**) The CS-$\delta^{15}N$ anomalies presented in this study reveal a decadal cyclicity that is not observed in the bulk sediment and deep-sea coral $\delta^{15}N$ records. Anomalies were calculated by subtracting the mean $\delta^{15}N$ value of each individual record. CS-$\delta^{15}N$ records were smoothed with an 8-year Gaussian filter. RT10 and RT4 are two cores collected from individual colonies at Palmyra Atoll (fig. S14).

(Fig. 1C). Rather, Palmyra most directly receives nitrogen from a nearby upwelling at ~10°N (Fig. 1C) (*29*) owing to a combination of Ekman pumping, friction between the westward-flowing North Equatorial Current (NEC) and the eastward-flowing North Equatorial Countercurrent (NECC), and meridional circulation (*30*, *31*). The upwelling water derives from the westernmost arm of the thermocline "shadow zone," which is characterized by high-$\delta^{15}N$, high-$\delta^{18}O$ nitrate; a strong nitrogen-to-phosphorus deficit; high nitrite concentration; and proteomic signs of nitrite reduction, demonstrating its connectivity with the ETNP ODZ (Fig. 1D) (*29*, *32*, *33*). This upwelling therefore links the CS-$\delta^{15}N$ of the Palmyra corals to the main ETNP ODZ. In addition, the controls on the upwelling near Palmyra are linked to the same band of easterlies that causes upwelling over the main ODZ (*31*). With this network of corals, we investigated the history and regional influence of ETNP suboxia over the last 80 years.

Replicate monthly CS-$\delta^{15}N$ records, when aligned by using coral $\delta^{18}O$ (a mixed proxy of temperature and salinity), show high fidelity between different parts of the same colony and between different colonies, highlighting the robustness of CS-$\delta^{15}N$ as a recorder of environmental signals (Fig. 3). On average, both the existing sediment $\delta^{15}N$ records and our new scleractinian coral–bound $\delta^{15}N$ records have values that are intermediate between the mean global pycnocline $\delta^{15}N$ of nitrate (~6.2‰) (*12*) and the value found in the core of the ODZ (≥15‰) (Fig. 2A). This suggests that all locations are influenced regionally by the ODZ, highlighting the potential of these records to track historical changes in oxygenation. The composite scleractinian coral CS-$\delta^{15}N$ timeseries covering the last 80 years is, in its apparent longterm structure, arguably similar to the ETNP sediment and Hawaiian deep-sea coral $\delta^{15}N$ records, with a decline over the 20th century (Fig. 2B). At shorter timescales, however, the coral CS-$\delta^{15}N$ is very different from that of the other ETNP $\delta^{15}N$ records. Specifically, we observe multiple positive CS-$\delta^{15}N$ excursions (of >1‰), approximately centered on years 1950, 1957, 1975, 1990, 2001 and 2012, that last less than 10 years each (Fig. 2B). The coral records thus reveal a strong decadal periodicity in WCD (fig. S1). The CS-$\delta^{15}N$ records from the ODZ region and from the Central Pacific share 74% and 67-86% of their variance, respectively (figs. S2, S3), demonstrating that the recorded changes are not site-specific but rather reflect regional oceanographic processes.

The high-resolution CS-$\delta^{15}N$ records reported here provide insight into the mechanisms regulating suboxia in the ETNP. The CS-$\delta^{15}N$ maxima (interpreted as peaks in ETNP denitrification) coincide with North Pacific cool phases of Pacific Decadal Variability (PDV) (*34*) (Fig. 4). A cool PDV phase is characterized by lower sea surface temperature over the North Pacific (north of 20°N) and stronger tropical winds across the Pacific basin (i.e., the easterlies), along the California coast (i.e., the California Current System) and across the Sierra Madre Mountain Range (i.e., the gap-wind jets). These key regions respond synchronously to atmospheric forcing over the North Pacific, leading to periods of intense wind-driven upwelling that bring the thermocline closer to the surface, enriching the surface water in nutrients, stimulating primary production, and increasing the export of organic matter to the ETNP thermocline (fig. S4). We infer that this increases oxygen demand in the ETNP shadow

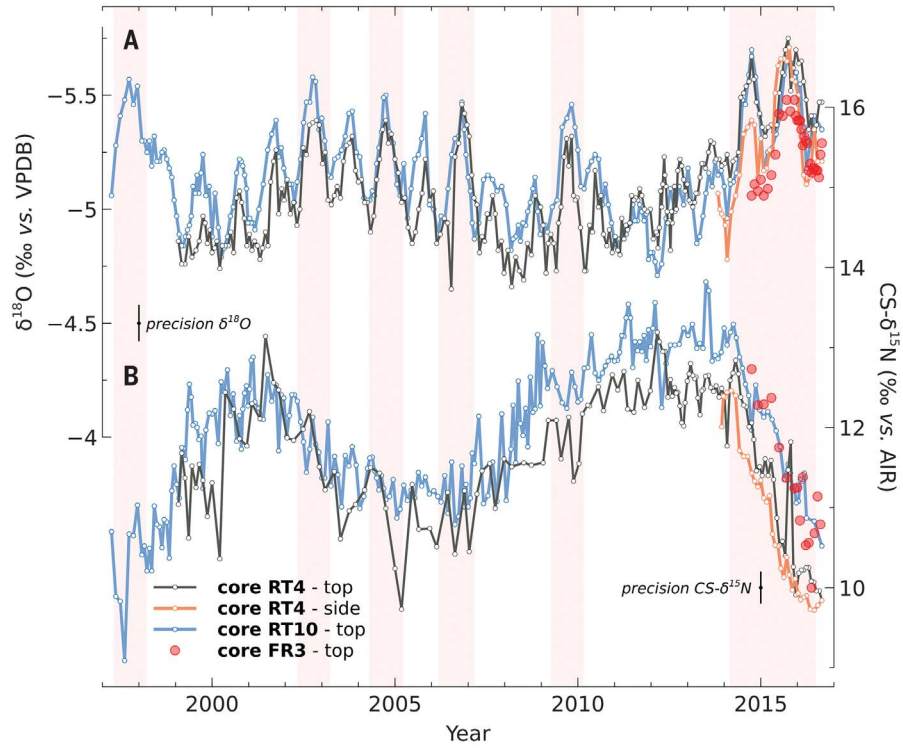

Fig. 3. The intercolony fidelity of monthly resolved geochemical proxies in the genus *Porites* was assessed by comparing records from three different colonies (RT4, RT10, and FR3), and the intracolony fidelity was assessed by comparing a record from the top and a record from the side of colony RT4. (**A**) A strong seasonal and interannual (El Niño events, red shading) cyclicity can be seen in the coral skeleton $\delta^{18}O$ records $\delta^{18}O$ is expressed as per mille, normalized versus the Vienna Peedee Belemnite isotope reference (‰ vs. VPDB). (**B**) The interannual variability is absent from the CS-$\delta^{15}N$ record, which is characterized instead by a strong decadal variability. The correlation between the records presented here is further examined in fig. S2.

zone and thus causes the ODZ to expand and WCD to intensify.

The overall tight coupling between decadal oscillations in WCD and the thermocline depth (Fig. 4) is consistent with two previously proposed contributors to eastern Pacific ODZ variability: (i) stronger easterlies can increase upwelling, biological productivity, and organic matter export to depth, causing the ODZ to expand and WCD to accelerate (*35*, *36*); and (ii) shoaling of the thermocline can bring the thermocline's "shadow zone" of slower ventilation closer to the surface, causing more respiration of sinking organic matter to occur within suboxic waters, also accelerating WCD. However, the correlation between CS-$\delta^{15}N$ and thermocline depth changes is not perfect (Fig. 4), and there may also be other contributors to the observed ODZ variation, including processes that involve teleconnections. The most powerful modes of the PDV are the Pacific Decadal Oscillation (PDO, the first principal component of the sea surface temperature anomaly north of 20°N) (*37*) and the North Pacific Gyre Oscillation (NPGO, the second dominant mode of sea surface height variability over 180° to 160°W, 25° to 62°N) (*38*). These indices capture modes of spatiotemporal change in SST and, thus, also in winds, upwelling, and thermocline depth (fig. S5). Upwelling and primary production will depend on the respective phases of the NPGO and PDO as well as their interaction (fig. S6). These changes vary spatially, implying that the size of the ETNP ODZ and the WCD rate are potentially sensitive not only to local changes in productivity and ventilation but also to more distal changes. Such changes may, for example, impact the oxygen content of the water that advects into or mixes with the ETNP ODZ (*39*).

The CS-$\delta^{15}N$ observations have implications for a range of hypotheses for the decadal controls on the ETNP ODZ. The finding of a linkage of increased WCD with cold anomalies in North Pacific surface waters is counter to previous predictions (*1*, *3*) that focus on the expectation that, in a warmer world, O_2 solubility would decrease, and stratification would strengthen, leading to slower resupply of oxygen to the ODZs (*2*). Moreover, our coral records contradict the prediction of numerical model simulations, that the enhanced surface productivity and subsurface oxygen demand of the negative (cool, high upwelling) phase of the PDO would be overwhelmed by the associated strengthening of the Equatorial Undercurrent (EUC) that imports oxygen to the ETNP (*40*, *41*). In this prediction, denitrification in the ODZ would hold constant or decline during the high-upwelling (i.e., negative) phase of the PDO, contrary to our data (Fig. 4). Rather, our coral records suggest that the strength of the EUC does not exert a strong feedback on the ODZ at decadal timescales (fig. S7A). A change in the oxygen concentration of the North Pacific Current (NPC), which feeds the California Current System, has also been proposed to modulate the dissolved oxygen content in the ETNP by altering the ventilation of the North Pacific subtropical gyre (*42*). However, the North Pacific Gyre Oscillation Index (NPGO, a proxy for O_2 supply to the NPC) shows increased O_2 supply (i.e., positive NPGO phases) during periods of increased WCD (i.e., greater suboxia) (fig. S7B) suggesting that this ventilation pathway does not drive the observed WCD changes. The El Niño-Southern Oscillation (ENSO) is thought to be another major cause of WCD variability in the Eastern Tropical Pacific. Hindcast simulations suggest that, during La Niña events, WCD rates are up to 70% higher in response to shoaling of the upper boundary of the ODZ, a response to stronger easterlies (*43*). However, we did not find evidence of such changes in our finely resolved (monthly to subannual) network of coral records (Fig. 4). The fact that ENSO-driven modulation of WCD is not recorded in the coral records may be, at least partly, due to the decades-long residence time of nitrate in the ODZs (*44*), which would dampen the effect of interannual changes on ODZ nitrate $\delta^{15}N$ and, thus, on the CS-$\delta^{15}N$ records. In general, however, the lack of ENSO-driven variability in our CS-$\delta^{15}N$ records leaves unproven the model-supported hypothesis that ENSO causes large oscillations in suboxia and WCD rate.

The high-resolution CS-$\delta^{15}N$ records clarify the ODZ baseline for any changes due to global warming. Recent expansion of the ETNP ODZ has been inferred from ship measurements from years 1972, 1994, 2007, and 2012 (*5*), with a major change observed between 2007 and 2012. Data on the cumulative ODZ-integrated nitrite concentration (a proxy for WCD) from these discrete sampling intervals agrees well with our CS-$\delta^{15}N$ reconstruction of ODZ variation (white circles, Fig. 4A). However, our continuous record indicates that the differences among these four discrete measurements can be attributed to decadal ODZ oscillations. The first three historical measurements took place during excursions to lower CS-$\delta^{15}N$ and, hence, lower denitrification associated with weaker wind-driven upwelling indices (e.g., positive PDO phases), whereas the 2012 observations coincided with a peak in CS-$\delta^{15}N$ and, hence, high denitrification at the climax of stronger upwelling indices (e.g., the negative PDO phase) (Fig. 4B). This aliasing by the strong decadal-scale variability of the ODZ led to the inference that the ODZ

has undergone a secular expansion over recent decades. More broadly, although our CS-δ^{15}N composite records do not show a clear global warming–induced trend in the ODZ over the last 80 years, the gradual δ^{15}N decline observed in Hawaiian proteinaceous corals and ETNP sediments over the 20th Century (*10*, *17*) is not falsified by the CS-δ^{15}N data. However, if there was such a trend, then it appears to have been reversed in recent decades. Conversely, the strong decadal δ^{15}N variations evident in CS-δ^{15}N are not apparent in the other records. Future generation of CS-δ^{15}N records from before 1940 will shed light on the history of and controls on the ODZs at the centennial time scale.

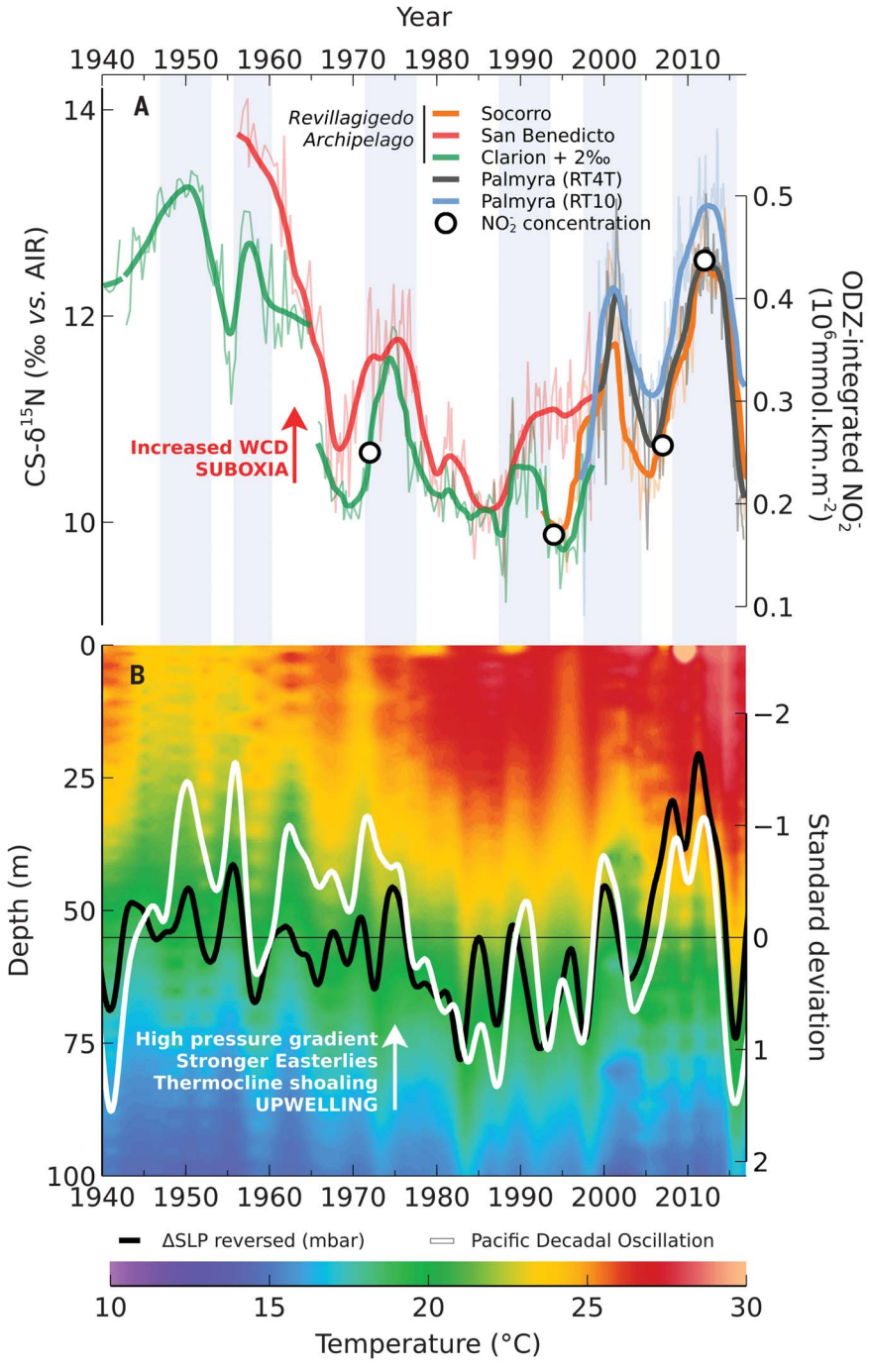

Fig. 4. In the Eastern Tropical North Pacific ODZ, suboxia is modulated on decadal timescales by bacterial oxygen demand, which is in turn fueled by wind-driven upwelling. (**A**) Events of enhanced suboxia are indicated by shaded areas and correspond to phases of elevated CS-δ^{15}N and ODZ-integrated nitrite concentration (white circles) (*5*), both proxies for WCD. The justification for the +2‰ offset applied to the Clarion record is provided in the supplementary text. (**B**) The PDO (white line), a component of North Pacific Decadal Variability, influences the low-frequency temperature variability within the ODZ: 10° to 25°N, 90° to 120°W (colorized raster, data source: World Ocean Database) and sea level pressure gradients between the Eastern and Western Pacific [ΔSLP, HadSLP2 (*47*), black line], which affects the strength of the easterlies. All time series were smoothed with an 8-year Gaussian filter, represented by bold lines.

Implications for the future of the ETNP ODZ

The discovery of strong decadal ODZ variation, best explained by wind-driven changes in upwelling, offers a new perspective on the possible future of the ETNP ODZ. Specifically, any global warming–driven trend in the ODZ will be strongly overprinted by decadal variation. Given our findings, improved forecasting of PDV would provide a degree of predictability to future ODZ changes. In this context, we expect that the recent onset of extremes in PDV (fig. S6) will manifest in correspondingly large changes in Eastern Tropical Pacific oxygen deficiency, potentially impacting marine ecosystems along the western American coast (*45*, *46*).

REFERENCES AND NOTES

1. L. Stramma, G. C. Johnson, J. Sprintall, V. Mohrholz, *Science* **320**, 655–658 (2008).
2. R. E. Keeling, A. Körtzinger, N. Gruber, *Annu. Rev. Mar. Sci.* **2**, 199–229 (2010).
3. S. Schmidtko, L. Stramma, M. Visbeck, *Nature* **542**, 335–339 (2017).
4. S. J. Bograd *et al.*, *Geophys. Res. Lett.* **35**, 1–6 (2008).
5. R. E. A. Horak, W. Ruef, B. B. Ward, A. H. Devol, *Geophys. Res. Lett.* **43**, 5252–5260 (2016).
6. J. J. M. Busecke, L. Resplandy, S. J. Ditkovsky, J. G. John, *AGU Adv.* **3**, e2021AV000470 (2022).
7. L. Bopp *et al.*, *Biogeosciences Discuss.* **10**, 3627–3676 (2013).
8. T. L. Frölicher *et al.*, *Global Biogeochem. Cycles* **34**, 1–20 (2020).
9. W. Fu, F. Primeau, J. Keith Moore, K. Lindsay, J. T. Randerson, *Global Biogeochem. Cycles* **32**, 551–564 (2018).
10. C. Deutsch *et al.*, *Science* **345**, 665–668 (2014).
11. J. D. Cline, I. R. Kaplan, *Mar. Chem.* **3**, 271–299 (1975).
12. F. Fripiat *et al.*, *Nat. Geosci.* **14**, 855–861 (2021).
13. M. A. Altabet *et al.*, *Deep Sea Res. Part I Oceanogr. Res. Pap.* **46**, 655–679 (1999).
14. D. M. Sigman, P. J. DiFiore, M. P. Hain, C. Deutsch, D. M. Karl, *Geophys. Res. Lett.* **36**, 2008GL035784 (2009).
15. J. A. Brandes, A. H. Devol, *Global Biogeochem. Cycles* **16**, 1–14 (2002).
16. J. R. Luyten, J. Pedlosky, H. Stommel, *J. Phys. Oceanogr.* **13**, 292–309 (1983).
17. O. A. Sherwood, T. P. Guilderson, F. C. Batista, J. T. Schiff, M. D. McCarthy, *Nature* **505**, 78–81 (2014).
18. X. T. Wang *et al.*, *Earth Planet. Sci. Lett.* **400**, 243–250 (2014).
19. C. E. Tems, W. M. Berelson, M. G. Prokopenko, *Geophys. Res. Lett.* **42**, 419–427 (2015).
20. S. Moretti *et al.*, Analytical improvements and assessment of long-term performance of the oxidation-denitrifier method. *Rapid Commun. Mass Spectrom.* (2023), doi: 10.22541/au.168616993.39320235/v1.
21. X. T. Wang *et al.*, *Geochim. Cosmochim. Acta* **148**, 179–190 (2015).
22. F. Houlbrèque, C. Ferrier-Pagès, *Biol. Rev. Camb. Philos. Soc.* **84**, 1–17 (2009).
23. R. Grover, J.-F. Maguer, D. Allemand, C. Ferrier-Pagés, *Limnol. Oceanogr.* **48**, 2266–2274 (2003).
24. X. T. Wang *et al.*, *Earth Planet. Sci. Lett.* **441**, 125–132 (2016).
25. A. Martínez-García *et al.*, *Geochem. Geophys. Geosyst.* **23**, e2022GC010396 (2022).
26. A. S. Studer *et al.*, *Paleoceanogr. Paleoclimatol.* **36**, e2020PA004063 (2021).
27. N. N. Duprey *et al.*, *Glob. Chang. Biol.* **26**, 1338–1353 (2020).
28. N. N. Duprey *et al.*, *Mar. Pollut. Bull.* **120**, 109–116 (2017).
29. D. Marconi *et al.*, Distinguishing the isotopic signals of nitrate assimilation and denitrification along meridional Pacific section US GEOTRACES GP15, ESS Open Archive (2024); https://10.22541/essoar.173144359.93122438/v1.

30. J. P. McCreary, P. Lu, *J. Phys. Oceanogr.* **24**, 466–497 (1994).
31. A. Capotondi, B. Qiu, *J. Clim.* **36**, 1001–1015 (2023).
32. P. A. Rafter, D. M. Sigman, *Limnol. Oceanogr.* **61**, 14–31 (2016).
33. M. A. Saito *et al*., *Nat. Geosci.* **13**, 355–362 (2020).
34. A. Capotondi *et al*., *Nat. Rev. Earth Environ.* **4**, 754–769 (2023).
35. C. Deutsch, H. Brix, T. Ito, H. Frenzel, L. Thompson, *Science* **333**, 336–339 (2011).
36. T. Ito, M. C. Long, C. Deutsch, S. Minobe, D. Sun, *Global Biogeochem. Cycles* **33**, 110–124 (2019).
37. N. J. Mantua, S. R. Hare, Y. Zhang, J. M. Wallace, R. C. Francis, *Bull. Am. Meteorol. Soc.* **78**, 1069–1079 (1997).
38. E. Di Lorenzo *et al*., *Geophys. Res. Lett.* **35**, 2007GL032838 (2008).
39. A. Margolskee, H. Frenzel, S. Emerson, C. Deutsch, *Global Biogeochem. Cycles* **33**, 875–890 (2019).
40. O. Duteil, A. Oschlies, C. W. Böning, *Biogeosciences* **15**, 7111–7126 (2018).
41. M. A. Poupon, L. Resplandy, M. Lévy, L. Bopp, *Geophys. Res. Lett.* **50**, e2022GL102123 (2023).
42. M. Pozo Buil, E. Di Lorenzo, *Geophys. Res. Lett.* **44**, 4204–4213 (2017).
43. S. Yang, N. Gruber, M. C. Long, M. Vogt, *Global Biogeochem. Cycles* **31**, 1470–1487 (2017).
44. T. Ito, C. Deutsch, *Geophys. Res. Lett.* **37**, 2009GL041595 (2010).
45. D. Breitburg *et al*., *Science* **359**, eaam7240 (2018).
46. C. Deutsch, J. L. Penn, N. Lucey, *Annu. Rev. Mar. Sci.* **16**, 217–245 (2024).
47. R. Allan, T. Ansell, *J. Clim.* **19**, 5816–5842 (2006).
48. N. N. Duprey *et al*., Coral isotopes records & Linear Extension Rates, Dryad (2024); https://doi.org/10.5061/dryad.x95x69ptd.

ACKNOWLEDGMENTS

This work is dedicated to our esteemed and dearly missed colleagues P. J. Crutzen and J. D. Carriquiry without whom this project would not have been possible. We thank M. Schmidt, B. Hinnenberg, M. Dumestre, J. Jung, E. J. Drenkard, M. Pozo-Buil, C. Menkes, S. Cravatte, M. Meffert, and P. Salinas-de-León. In addition, we are grateful to The Nature Conservancy, the U.S. Fish and Wildlife Service, and the Palmyra Atoll Research Consortium for logistical support and access to the refuge (special use permit 12533-16024). We thank G. G. V. Rousseau and D. Saldierna for the access to the Parque Nacional Revillagigedo and the crew of the S/Y Acadia, R. Dodwell and G. Dodwell, for logistical support. The field campaign at Socorro Island was led under the salvoconducto granted by the Mexican authorities to the project "Influencias de la variación ambiental sobre ecosistemas de arrecife coralino." We are grateful for the constructive comments and suggestions provided by four anonymous reviewers that contributed to improve the manuscript. **Funding:** The Max Planck Society (G.H.H., H.V., and A.M.G.); The Deutsche Forschungsgemeinschaft (DFG, German Research Foundation), project no. 468591845 - SPP 2299/project no. 441832482 (A.M.G.); Paul Crutzen Postdoctoral fellowship (N.N.D.); U.S. NSF grants OCE1736652 and OCE2049416 (D.M.S.). **Author contributions:** Conceptualization: N.N.D., C.D.C., and A.M.G.; Methodology: N.N.D., A.D.F., J.D.C., S.C.S., F.R., R.R., and A.M.G.; Investigation: N.N.D. and A.D.F.; Visualization: N.N.D., D.M., and A.M.G.; Funding acquisition: G.H.H., A.M.G., and M.R.; Project administration: N.N.D. and A.M.G.; Supervision: A.M.G.; Writing – original draft: N.N.D. and A.D.F.; Writing – review and editing: N.N.D., A.D.F., J.D.C., C.D.C., S.C.S., H.V., F.R., R.R., D.M., D.M.S., G.H.H., A.M.G., M.R., and H.R.B. **Competing interests:** The authors declare that they have no competing interests. **Data and materials availability:** All coral geochemical records are available on Dryad (*48*).

SUPPLEMENTARY MATERIALS

science.org/doi/10.1126/science.adk4965
Materials and Methods
Supplementary Text
Figs. S1 to S14
Table S1
References (*49*–*72*)

Submitted 31 October 2023; accepted 28 October 2024
10.1126/science.adk4965